Research Square

Preprints are preliminary reports that have not undergone peer review.
They should not be considered conclusive, used to inform clinical practice,
or referenced by the media as validated information.

The Effect of Copper Addition to Secondary Aluminum Obtained from Aluminum Dross and Casting Temperature on Fluidity and Microstructural Properties

Selçuk Yeşiltepe

selcukyesiltepe@osmaniye.edu.tr

İbrahim Umut Yurtsever

Research Article

Keywords: Aluminum dross, Secondary aluminum, Fluidity, Microstructure, Hardness

Posted Date: November 13th, 2026

DOI: https://doi.org/10.21203/rs.3.rs-11427843/v1

License: This work is licensed under a Creative Commons Attribution 4.0 International License.
Read Full License

Additional Declarations: No competing interests reported.

The Effect of Copper Addition to Secondary Aluminum Obtained from Aluminum Dross and Casting Temperature on Fluidity and Microstructural Properties

Selçuk Yeşiltepe*, İbrahim Umut Yurtsever

Osmaniye Korkut Ata University, Mechanical Engineering Department

***Corresponding Author: selcukyesiltepe@osmaniye.edu.tr**

ABSTRACT

In this study, the effects of copper addition and casting temperature on the fluidity and microstructural properties of secondary aluminum recovered from dross waste generated during aluminum production were investigated. In this context, alloys containing different copper contents (0%, 1%, and 2.5%) were processed at casting temperatures of 700, 725, and 750 °C, and the fluidity performances of the alloys were evaluated using the spiral mold method. The microstructural properties of the obtained samples were examined using scanning electron microscopy (SEM) and energy-dispersive X-ray spectroscopy (EDS), and microhardness measurements were performed. The results showed that copper addition and casting temperature jointly affected the fluidity behavior. While the highest fluidity lengths in the samples without copper addition and containing 1% Cu were measured as 17.6 and 17.0 cm, respectively, at 750 °C, the highest value in the sample containing 2.5% Cu was determined as 15.7 cm at 725 °C. Microstructural examinations revealed that, with copper addition, the morphology of the secondary phases transformed from needle-like and plate-like structures into a eutectic-dendritic network and coarser, band-like structures. The findings indicate that the casting performance of dross-derived secondary aluminum can be improved by controlling the alloy composition and process temperature.

Keywords: Aluminum dross, Secondary aluminum, Fluidity, Microstructure, Hardness

INTRODUCTION

Aluminum dross generated during industrial aluminum production and casting processes is classified as hazardous waste due to its adverse effects on the environment and human health [1]. The reaction of this waste with moisture in storage areas leads to the release of toxic gases, particularly ammonia gas released as a result of the hydrolysis of aluminum nitride (AlN) in its structure [2], [3]. Sustainable environmental policies and circular economy requirements necessitate the recovery of these secondary wastes as value-added raw materials or engineering materials beyond their disposal [1], [3]. Physical and chemical characterization studies of aluminum dross have shown that, as the particle size of granular dross decreases, the oxide (Al_2O_3) and salt contents increase, whereas the metallic aluminum content decreases [4]. Pyrometallurgical melting processes are widely used to recover metallic aluminum from dross, and the efficient separation of the resulting liquid metal depends on the matrix components and the control of impurity elements [1], [4]. In addition, secondary aluminum dross can also be utilized as an environmentally friendly co-reductant in various high-temperature processes, such as the recovery of iron from copper slag [5].

In high-temperature metallurgical processes, the separation of liquid metal droplets from the slag phase and their clean collection at the bottom depend on the wettability characteristics and density differences between the phases [5], [6]. In studies conducted to increase aluminum recovery from aluminum white dross, it was determined that the liquid aluminum alloy exhibited a distinct non-wetting behavior on a solid slag substrate in the temperature range of 973 K to 1373 K [6]. Due to this barrier formed by the aluminum oxide layer and the poor wetting behavior, the coalescence of molten droplets is restricted in systems where flux (slag-forming agent) is not used [6]. However, the addition of metallic copper (Cu) to the medium increases the density of the metal phase and, together with suitable flux additions, enables the complete separation of the liquid metallic Al-Cu alloy from the slag and its clean collection at the bottom [6].

The success of recovered or alloyed aluminum-based materials in component manufacturing directly depends on the fluidity parameter, defined as the ability of liquid metal to fill the mold cavity [7]. Fluidity is a complex system dynamic affected by metal properties such as the chemical composition of the alloy, viscosity, surface tension, inclusion content, and solidification range, as well as casting temperature, mold material, and heat transfer conditions [7], [8]. While increasing the casting temperature linearly increases the fluidity distance of liquid metal, excessively high temperatures can increase the gas-dissolving capacity of the liquid metal, leading to porosity defects and the formation of coarse microstructural constituents in the casting structure [7], [9]. Increasing the mold temperature or using mold materials with low thermal conductivity, such as plaster, considerably increases fluidity by slowing the heat transfer rate, whereas microscopic inclusions and oxide films in the liquid metal increase the effective viscosity and surface tension, thereby restricting fluidity in narrow channels [8], [10].

Unlike pure metals, the fluidity mechanism in alloy systems undergoes fundamental changes depending on the type and amount of alloying elements [8], [11]. The addition of copper (Cu) to the aluminum matrix widens the solidification temperature range (ΔT) of the alloy and leads to a semi-solid solidification mode [10], [12]. Along this expanded solidification range, crystal interlocking (dendrite coherency) and solid-phase accumulation occurring at the tip of the flowing metal stream physically stop the progression of the liquid melt, resulting in a clear decrease in the fluidity distance [8], [11], [12]. It has been reported in spiral fluidity tests that increases in the Cu content lead to decreases in overall fluidity performance due to the widening of the solidification range [11], [13]. In contrast, changing the grain size morphology in the microstructure or transforming it into a globular morphology plays a decisive role in fluidity performance by affecting the apparent viscosity and stopping mechanisms of the semi-solid suspension [9], [13].

Within the scope of this study, the castability and flow characteristics of aluminum obtained through pyrometallurgical methods from aluminum dross, which is of critical importance in terms of hazardous waste management and the circular economy, were investigated. Although the fluidity behavior of Al-Cu systems containing primary or standard alloying elements has been extensively addressed in the literature, studies on the fluidity of aluminum matrices recovered from dross are limited. Accordingly, the effects of adding copper at different ratios (0%, 1%, and 2.5% Cu) to dross-derived aluminum and the effects of these addition ratios on the fluidity performance of the alloy at different casting temperatures (700°C, 725°C, and 750°C) were systematically compared.

2. MATERIALS AND METHODS

2.1. Raw Materials

The Al dross used in the study was obtained from a local industrial manufacturing company. The chemical composition of the dross, determined as a result of the analysis, is given in Table 1. The results shown in Table 1 indicate that the dross was obtained from the production of Zn-alloyed 7104 series alloys.

Table 1. Chemical Composition of the Aluminum Dross Used in the Experiments

Al	Zn	Si	Fe	Mn	Cu	Others
87.46	11.02	0.79	0.38	0.22	0.11	0.02

KCl and NaCl, used as fluxes in the study, were purchased from Sözen Kimya in technical grade (min. 99%). A graphite crucible and a Protherm 1100 model muffle furnace were used to melt the dross. After the dross was melted, slag removal was performed by adding flux. Subsequently, Cu was added to prepare the alloys designed to contain 1 and 2.5% Cu, and the melt was held at the casting temperature for 20 minutes for homogenization before being poured into the spiral fluidity mold, the technical drawing of which is presented in Figure 1.

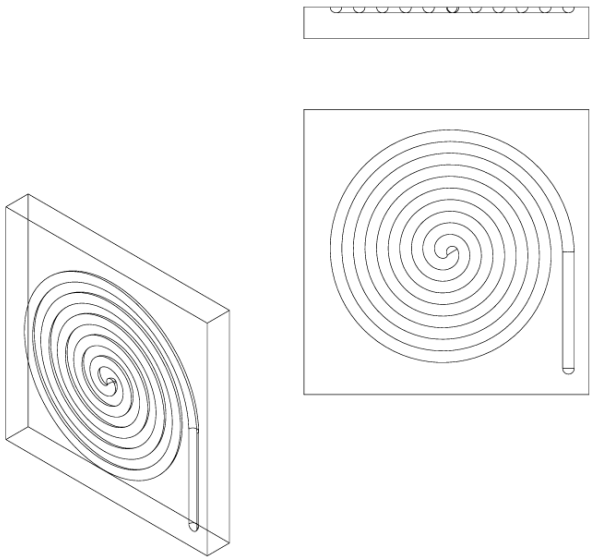


Figure 1. Technical Drawing of the Spiral Fluidity Mold

2.2. Characterization

The chemical composition of the obtained alloys was determined using Optical Emission Spectrometry (OES). The chemical composition of the cast alloys is given in Table 2.

Table 2. Chemical Composition of the Cast Aluminum Dross Alloy

Al	Zn	Si	Cu	Fe	Mn	Others
87.95	10.04	0,75	0,38	0,34	0,19	0,35

When Table 1, which shows the chemical composition of the raw material, is compared with Table 2, which contains the analysis results of the cast alloy, a slight decrease in the zinc (Zn) content of the dross during the melting and slag removal processes with flux can be observed. The high tendency of zinc to evaporate at increasing temperatures, the removal of a portion of it in the gas phase at high temperatures during pyrometallurgical melting, and its transfer into the slag structure through flux applications are considered the main reasons for this partial decrease.

The fluidity test results were determined by measuring the distance traveled by the alloys cast at the specified casting temperatures in the mold before completely solidifying. SEM/EDS and optical microscopy images were obtained from samples taken from the material solidified as a result of the fluidity test. HV0.5 microhardness measurements were performed to determine the effect of alloying on the material hardness.

3. RESULTS AND DISCUSSION

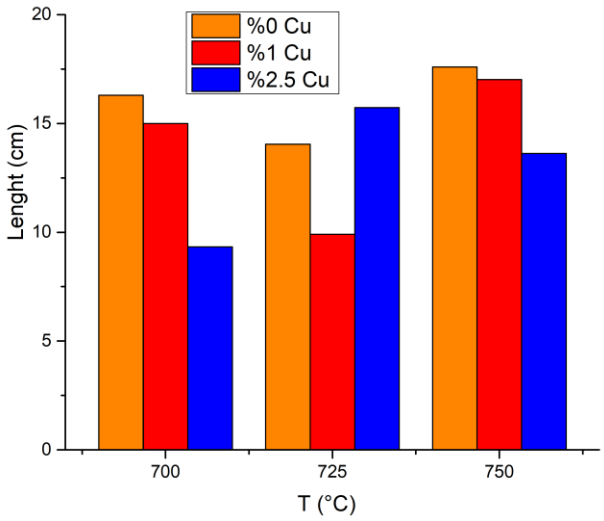


Figure 2. Variation in the fluidity length of secondary alloys obtained from aluminum dross as a function of different casting temperatures and copper contents.

According to the graph shown in Figure 2, in the sample without copper addition (0% Cu), the fluidity length, measured as 16.3 cm at 700 °C, decreased slightly to 14.1 cm at 725 °C, and reached its maximum value of 17.6 cm at a casting temperature of 750 °C as the liquid metal became superheated with increasing temperature. The high casting temperature reduced the dynamic viscosity of the melt, extended the time available for the solidification front to advance along the mold channel, and positively affected fluidity [8], [10].

A similar trend was observed in the alloy containing 1.0% Cu; the fluidity length decreased to its lowest value of 9.9 cm at 725 °C and then increased to 17.0 cm at 750 °C. In contrast, a different behavior emerged in the sample containing 2.5% Cu: while the lowest fluidity value (9.4 cm) was recorded at 700 °C, it reached 15.7 cm with a significant increase at a casting temperature of 725 °C, and then decreased to 13.6 cm at 750 °C.

The limitation of fluidity by a high copper content (2.5% Cu) at low temperatures (700 °C) can be explained by the widening of the solidification temperature range (solidus–liquidus difference) in the Al-Cu system and the nucleation of primary intermetallic phases (image) during liquid flow, which increases viscous resistance [8]. However, a temperature of 725 °C stands out as the casting temperature at which the melt viscosity and thermal energy reach an optimum balance for the secondary alloy containing 2.5% Cu.

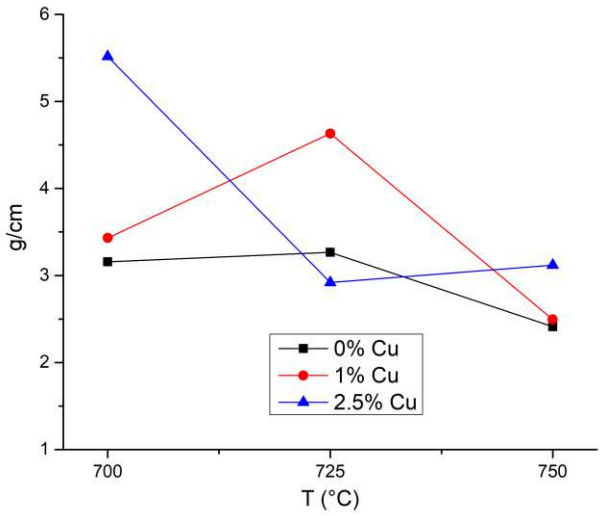


Figure 3. Mass per unit length (g/cm) values of fluidity channels cast at different casting temperatures and copper concentrations.

When the data obtained in Figure 3 are examined, an inversely proportional relationship is observed between the fluidity length and the mass per unit length (g/cm). At a casting temperature of 700 °C, the sample containing 2.5% Cu exhibited the highest mass per unit length, at 5.52 g/cm, despite having the shortest fluidity distance. This situation is associated with the high specific gravity of copper (image) and the complete filling of the mold cross-sectional area before the liquid flow stops.

At 725 °C, the highest mass per unit length was obtained in the sample containing 1.0% Cu (4.64 g/cm), in which the fluidity length was restricted. At the highest casting temperature of 750 °C, the mass per unit length values of all alloys converged and decreased to a lower range (2.41–3.12 g/cm). This decrease observed at high temperatures is explained by the solidification of the liquid metal along a thinner cross-section at the mold wall due to its high flow velocity, oxide inclusions increasing with temperature in dross-derived secondary aluminum melts, or solidification porosity.

The fact that the sample containing 2.5% Cu at a casting temperature of image exhibited the highest mass per unit length with image despite having the shortest fluidity distance (9.4 cm) is noteworthy in terms of hydrodynamic flow and cross-sectional filling characteristics. This situation is explained by the liquid flow being stopped at an early stage before it can advance along the channel due to the high dynamic viscosity of the melt and the widening solidification range at a low casting temperature [8]. However, before the flow stopped, the channel cross-sectional area was completely and densely filled in the transverse direction due to the high specific gravity of copper (image) and the effect of dense intermetallics. This dense mass transfer, which could not extend over long distances and was confined to a short path, caused the linear mass per unit length to reach its maximum level. In contrast, at high temperatures such as image,

the increase in the flow velocity of the melt and its progression along the channel in the form of a thinner cross-section triggered a decrease in the mass per unit length values [8].

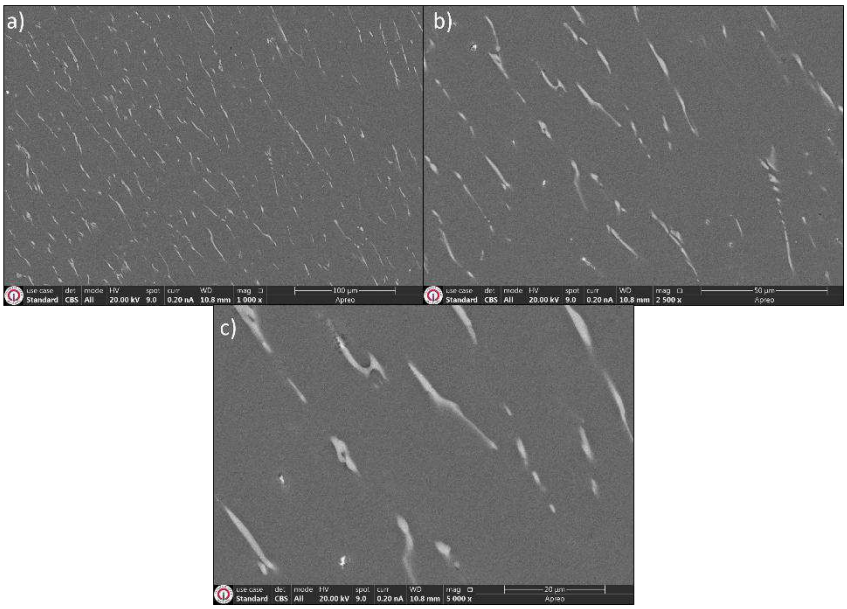


Figure 4. SEM microstructure images of the secondary aluminum sample without copper addition (0% Cu): a) 1000×, b) 2500×, and c) 5000× magnification.

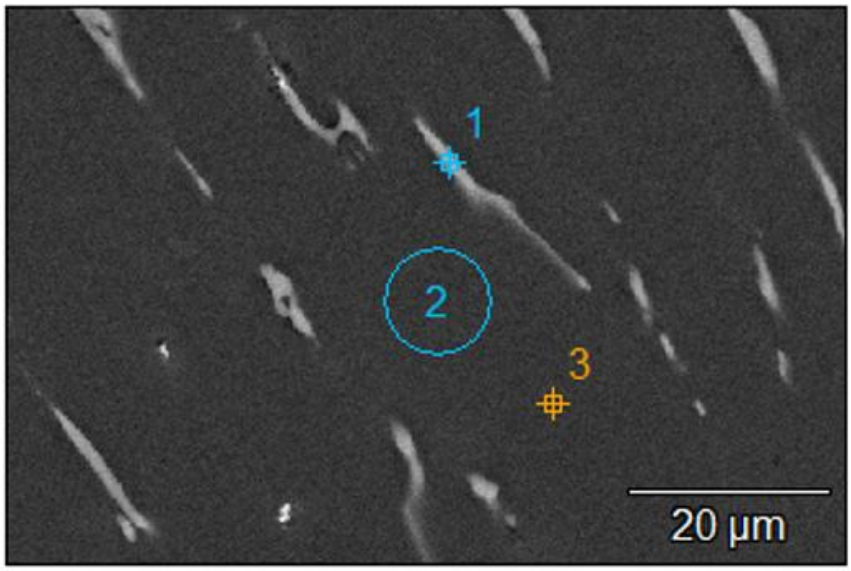


Figure 5. SEM microstructure image and EDS analysis points of the secondary aluminum sample without copper addition (0% Cu).

Table 3. EDS Point Analysis Results Obtained from the Unalloyed (0% Cu) Secondary Aluminum Sample (wt.%).

Analysis Point	Mg	Al	Mn	Fe	Cu
1	1.26	83.34	4.37	11.03	-
2	-	-	-	-	-
3	1.13	97.98	0.68	-	0.21

The SEM microstructure images at different magnifications, elemental analysis points, and energy-dispersive X-ray spectroscopy (EDS) results expressed in weight percent (wt.%) obtained from these points for the secondary aluminum alloy without copper addition (0% Cu), obtained by melting aluminum dross, are presented in Figures 4 and 5 and Table 3, respectively.

Microstructural examinations performed using SEM revealed that secondary phases with a light-colored (bright) contrast were aligned parallel to the solidification and liquid metal flow directions and exhibited orientation throughout the matrix within the image-Al solid solution matrix. In the high-magnification images (see Figure 4b, c), it becomes evident that these phases have a discontinuous, fractured, needle-like, and plate-like morphological structure [14].

The point EDS analyses performed to verify the qualitative and quantitative compositions of the phases (see Figure 5 and Table 3) support the microstructural observations. The concentrations of 11.03% Fe and 4.37% Mn detected in the Point 1 analysis obtained from the light-colored needle-like precipitate indicate that the Fe and Mn impurities present in the dross-derived secondary aluminum melt form Fe-Mn-rich intermetallic precipitates (image or image-image derivatives) in the interdendritic regions during solidification [14], [15].

In contrast, the Point 3 analysis obtained from the dark-colored matrix region represents the primary image-Al solid solution, with a composition of 97.98 wt.% Al and 1.13 wt.% Mg. The presence of Mg in the matrix reflects the traces of secondary aluminum present in the recovered dross source [16].

These hard and brittle needle-like Fe-Mn-rich intermetallic phases, which precipitate between dendrite arms and become oriented along the flow direction during the solidification of the dross melt, increase viscous resistance during liquid metal progression. The distribution of these needle-like phases observed in the structure constitutes the fundamental microstructural mechanism underlying the fluidity limitations and mass per unit length (g/cm) variations exhibited by unalloyed dross melts during casting.

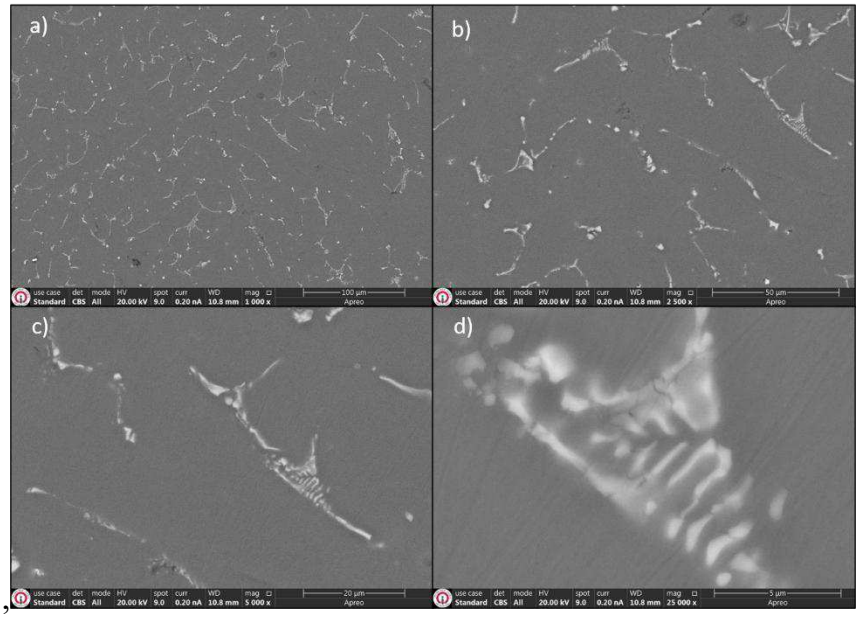


Figure 6. SEM microstructure images of the secondary aluminum sample with 1% Cu addition: a) 1000×, b) 2500×, c) 5000×, and d) 25000× magnification.

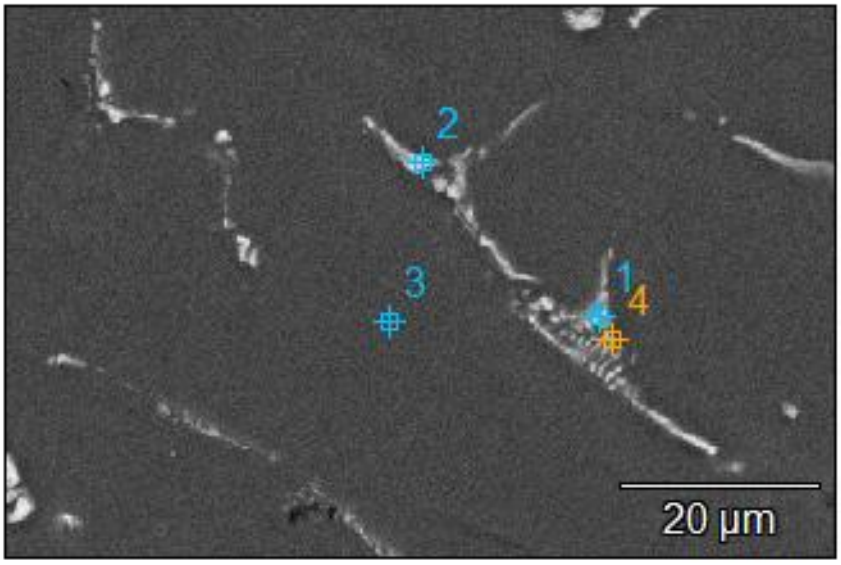


Figure 7. SEM microstructure image and EDS analysis points of the secondary aluminum sample with 1% Cu addition.

Table 4. EDS Point Analysis Results Obtained from the Secondary Aluminum Sample with 1% Cu Addition (wt.%).

Analysis Point	Mg	Al	Mn	Fe	Cu
1	1.28	87.44	2.83	7.94	0.51
2	1.17	80.70	3.88	14.26	-
3	1.01	81.80	4.12	13.07	-
4	1.04	98.06	0.89	-	-
5	0.95	81.36	3.78	13.77	0.16

The SEM microstructure images at different magnifications of the secondary aluminum alloy obtained by adding 1% Cu to the aluminum dross melt, the EDS analysis locations on the microstructure, and the elemental composition data expressed in weight percent (wt.%) obtained from these points are shown in Figures 6 and 7 and Table 4, respectively.

SEM microstructural examinations (see Figure 6a–d) clearly show that the addition of copper to the melt significantly transforms the phase morphology during solidification. In contrast to the distribution of oriented needle-like and plate-like precipitates observed in the unalloyed sample (0% Cu), it was determined that the secondary phases in the alloy containing 1% Cu branched along the grain boundaries and between the primary image-Al dendrite arms, forming eutectic and fishbone-like (dendritic/eutectic-like) network structures. In the high-magnification images (see Figure 6c, d), this branched morphology is observed to progress as a continuous line, becoming confined within narrow interdendritic regions during the final stages of solidification.

The results of point EDS spectroscopy obtained from critical regions of the microstructure (see Figure 7 and Table 4) confirm the elemental characteristics of this solidified network phase structure. The analysis obtained from Point 4 represents the primary image-Al solid solution matrix, largely free of impurities, with a composition of 98.06 wt.% Al and 1.04 wt.% Mg. In the analyses obtained from Points 1, 2, 3, and 5 in different regions of the dendritic network structure, high Fe concentrations ranging from 7.94% to 14.26% and Mn concentrations ranging from 2.83% to 4.12% were measured. This demonstrates that the presence of copper in the melt affects the solidification range and promotes the precipitation of Fe- and Mn-based intermetallic phases in a eutectic-like morphology, forming networks along the peripheries of the primary dendrite arms [14], [17]. Furthermore, the Cu concentrations of 0.51% and 0.16% detected in the analyses of Points 1 and 5, respectively, indicate that a portion of the added copper has begun to incorporate into the peripheries of the intermetallic phases, forming complex compounds.

These dendritic Fe-Mn-rich intermetallic structures, which solidify as a continuous network between grain boundaries and dendrite arms, narrow the effective flow channels of the liquid metal advancing within the mold cavity and increase hydrodynamic frictional resistance. This eutectic-dendritic transformation identified in the microstructure constitutes the fundamental

microstructural mechanism underlying the variations in fluidity distance and fluctuations in mass per unit length (g/cm) exhibited by the 1% Cu addition at different casting temperatures.

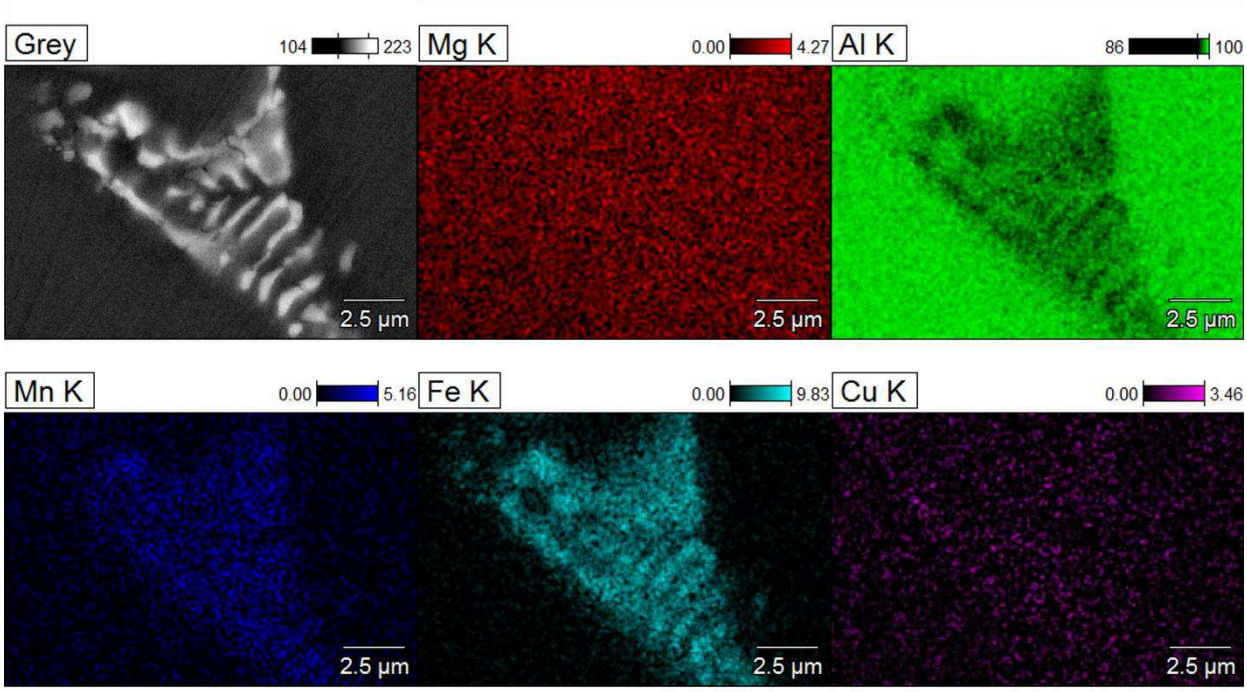


Figure 8. SEM image of the dendritic intermetallic phase region of the secondary aluminum alloy with 1% Cu addition and the corresponding EDS elemental mapping distributions: (a) reference SEM image, (b) Al, (c) Fe, (d) Mn, (e) Cu, and (f) Mg elemental maps.

The EDS elemental mapping analysis results performed to verify the elemental distribution and spatial clustering of the eutectic-dendritic secondary phases observed in the alloy with 1% Cu addition are presented in Figure 8. Examination of the elemental maps revealed that Fe and Mn elements were concentrated with a direct overlap on the light-colored precipitate morphology located between the primary image-Al dendrite arms. In contrast, the Al signal was observed to decrease in these intermetallic regions, while the Mg element exhibited a homogeneous distribution throughout the matrix. The Cu signal, represented by the purple color, was determined to exhibit local clustering at the peripheries of Fe-Mn-rich intermetallic phases, in addition to being dissolved within the matrix. These findings support the point EDS data and demonstrate that the addition of

1% Cu interacts with Fe and Mn impurities in the dross melt, forming a continuous intermetallic network structure at the grain boundaries [17].

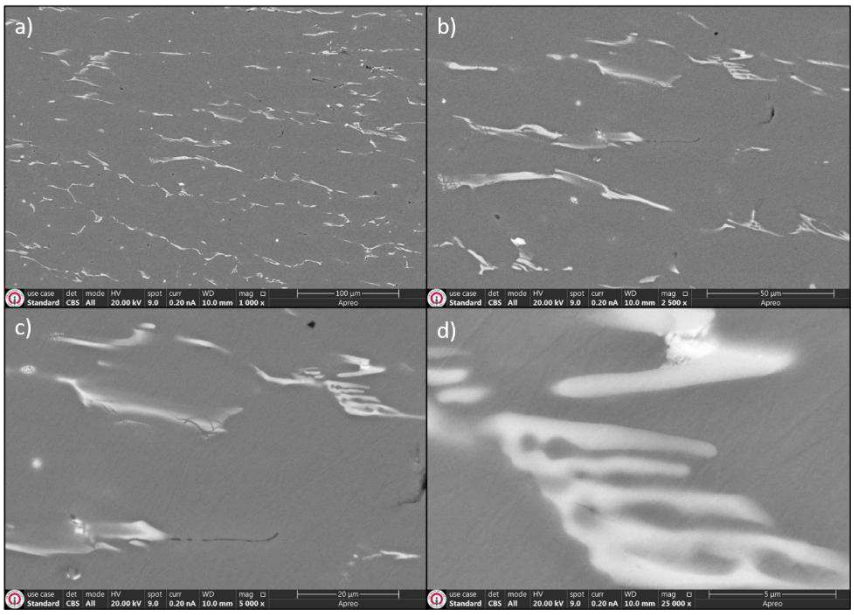


Figure 9. SEM microstructure images of the secondary aluminum sample with 2.5% Cu addition: a) 1000×, b) 2500×, c) 5000×, and d) 25000× magnification.

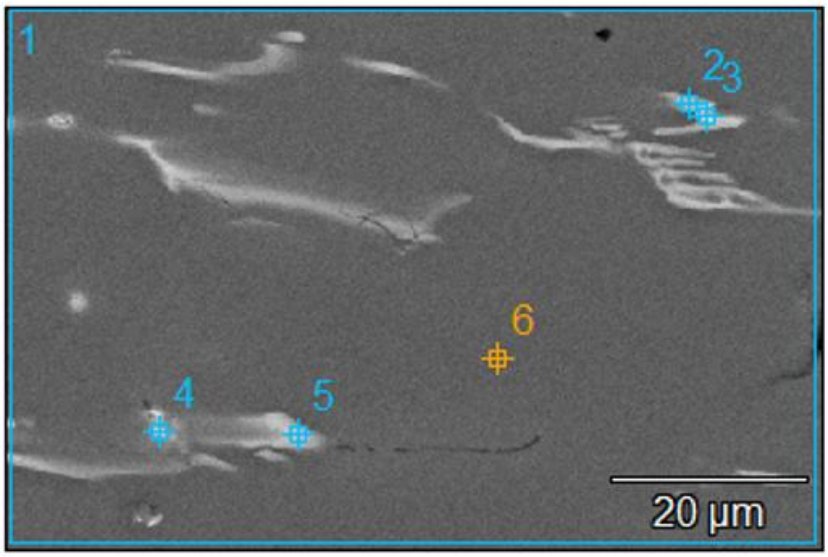


Figure 10. SEM microstructure image and EDS analysis points of the secondary aluminum sample with 2.5% Cu addition.

Table 5. EDS Point Analysis Results Obtained from the Secondary Aluminum Sample with 2.5% Cu Addition (wt.%).

Analysis Point	Mg	Al	Mn	Fe	Cu
1	1.49	96.11	0.86	0.81	0.72
2	1.55	84.90	3.69	7.88	1.98
3	5.86	74.31	0.93	2.57	16.33
4	4.15	73.67	1.78	4.06	16.35
5	5.22	76.58	5.02	11.62	1.55
6	1.00	98.33	0.67	-	-

The SEM microstructure images at different magnifications, elemental analysis points, and EDS results expressed in weight percent (wt.%) obtained from these points for the secondary aluminum alloy obtained by adding 2.5% Cu to the aluminum dross alloy are presented in Figures 9 and 10 and Table 5, respectively.

When the SEM microstructure images at different magnifications, elemental analysis points, and EDS results expressed in weight percent (wt.%) obtained from these points for the secondary aluminum alloy obtained by adding 2.5% Cu to the aluminum dross melt are examined, it is observed that the increasing copper content leads to a distinct phase evolution in the structure. In the microstructural examinations, unlike the needle-like structures in the unalloyed sample and the eutectic-dendritic network structure in the alloy containing 1% Cu, it was determined that the phases with bright contrast in the alloy containing 2.5% Cu formed coarser, more continuous, and band-like morphologies along the flow and solidification directions. In the high-magnification images, these bright phases located between the primary image-Al dendrite arms are observed to cluster as coarse precipitates as a result of eutectic reactions during the final stage of solidification.

Point EDS spectroscopy data obtained from different phase regions of the microstructure demonstrate that two main groups of secondary phases coexist in the structure. While the Point 6 analysis obtained from the dark-colored matrix region represents the primary image-Al solid solution free of impurities, with an Al content of 98.33% and an Mg content of 1.00%, high Cu concentrations of 16.33% and 16.35% were measured in the analyses obtained from Points 3 and 4, respectively, where the bright precipitates were prominent. This high copper content clearly confirms that the increasing Cu content in the melt leads to the formation of Cu-rich image (image eutectic phase), characteristic of cast aluminum alloys, or its complex Fe-Mn derivatives during the final moments of solidification [14], [17]. In addition, the analyses of Point 2 (7.88% Fe, 3.69% Mn, 1.98% Cu) and Point 5 (11.62% Fe, 5.02% Mn, 1.55% Cu) indicate that Fe and Mn impurities originating from the dross interact with Cu, incorporating a certain amount of Cu into Fe-Mn-rich complex intermetallic phases [18]. The increased Mg contents (4.15–5.86% Mg) detected at Points 3, 4, and 5 indicate the presence of complex secondary eutectic compounds composed of Al, Cu, Mg, Fe, and Mn elements at the peripheries of the secondary phases after solidification [15]. These high-volume-fraction Cu-rich image and complex Fe-Mn intermetallic precipitates, which form at

grain boundaries and between dendrites, increase the viscosity and hydrodynamic flow resistance of the liquid alloy, constituting the fundamental microstructural basis for the variations in fluidity distance and mass per unit length (g/cm) values measured depending on the casting temperature.

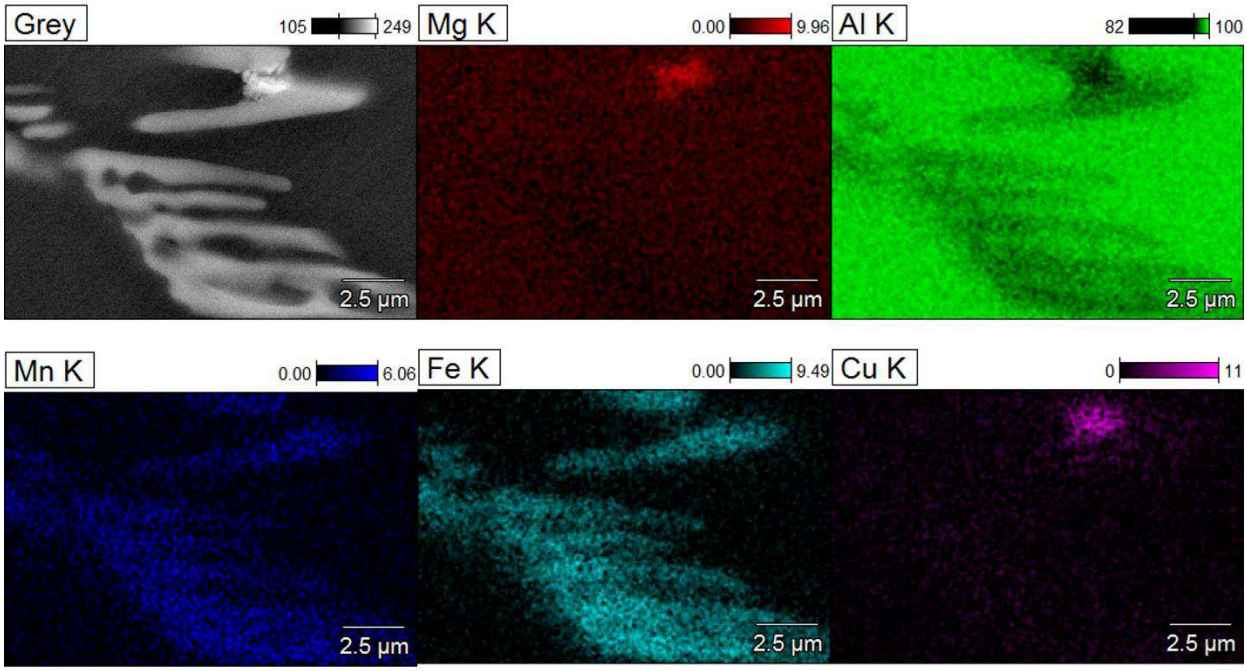


Figure 11. SEM image of the dendritic intermetallic phase region of the secondary aluminum alloy with 2.5% Cu addition and the corresponding EDS elemental mapping distributions: (a) reference SEM image, (b) Al, (c) Fe, (d) Mn, (e) Cu, and (f) Mg elemental maps.

The EDS elemental mapping analysis results performed to detail the microstructural phase distribution and elemental clustering behavior of the alloy cast by adding 2.5% Cu to the aluminum dross melt are presented in Figure 11. When the elemental distribution of the bright-morphology intermetallic phases extending between the eutectic dendrite arms is examined in the reference SEM image, it is determined that the Al signal exhibits high intensity in the matrix, while it locally decreases in the regions where the intermetallic phase is present. In contrast, the signals belonging to the Fe and Mn elements are observed to overlap directly and concentrate precisely on this bright intermetallic network, confirming that iron and manganese impurities originating from the dross form Fe-Mn-rich complex intermetallic precipitates during solidification [17]. In the copper map, where the color is represented by purple, it is clearly observed that, in addition to the partial distribution of the Cu signal throughout the solid-solution matrix, a localized, high-intensity bright cluster forms in the upper region of the intermetallic phase. This local Cu enrichment demonstrates that, with increasing copper content, Cu-rich image (image eutectic phase) or secondary phases derived from it nucleate at the boundaries of Fe-Mn intermetallic structures during the final moments of solidification [14], [18]. The Mg signal, represented in red, is generally distributed

uniformly throughout the matrix, while exhibiting a slight local concentration in the region where Cu clustering is observed; this is considered to indicate that complex eutectic reactions involving Al-Cu-Mg compositions occur at the end of solidification [15].

Table 6. HV0.5 microhardness results of secondary aluminum alloys as a function of different copper contents

Copper Content	Microhardness (HV0.5)	Standard Deviation (±)
%0 Cu	69	2,65
%1 Cu	72,5	3,65
%2.5 Cu	74,5	3,46

The effects of copper additions at different proportions (0%, 1%, and 2.5%) to the secondary aluminum alloy recovered from aluminum dross on the material microhardness (HV0.5) were investigated. Microhardness measurements were performed at 3 different points on the material surface under a load of 0.5 kgf, and the average HV0.5 measurement results are presented in Table 6 together with the standard deviation values. According to the HV0.5 measurement results, the average microhardness of the copper-free (0% Cu) sample was measured as image HV0.5. Subsequently, with the addition of 1% Cu to the alloy, the hardness value increased to image HV0.5. In the alloy in which the copper content was increased to 2.5%, the microhardness reached its maximum value of image HV0.5 with the increase in the volume fraction of Cu-rich image (image eutectic phase) and Fe-Mn-based complex intermetallic precipitates concentrated at the grain boundaries after solidification [19], [20].

This hardening behavior is directly related to the solid-solution strengthening provided by the added copper atoms within the matrix, in addition to the Fe and Mn impurities originating from the dross, and the inhibition of dislocation movement by the hard intermetallic phases precipitated at the grain boundaries [15], [21]. The needle-like structures in the undoped sample containing 0% Cu evolved into a eutectic and network-like morphology in the interdendritic regions with the addition of copper. First, the partial dissolution of copper atoms within the image-Al solid-solution matrix generated lattice strains, thereby providing solid-solution strengthening. Second, as also confirmed by SEM and EDS analyses, the Fe-Mn-rich phases exhibiting needle-like and plate-like characteristics in the undoped sample containing 0% Cu evolved into a continuous network and band morphology in the interdendritic regions with the addition of copper. At a Cu content of 2.5%, the volumetric density of image phases and complex intermetallics increased during the final stage of solidification [21]. These hard and brittle precipitates mechanically inhibited the sliding movement of dislocations during plastic deformation, significantly increasing the deformation resistance and microhardness of the material [19], [21].

4. CONCLUSIONS

The effects of copper additions at different proportions (0%, 1%, and 2.5% Cu) and casting temperatures (700, 725, and 750 °C) on the fluidity, microstructure, and hardness properties of a secondary aluminum alloy recovered from aluminum dross by pyrometallurgical methods were investigated.

1. Increasing the casting temperature generally increased the fluidity distance by reducing the dynamic viscosity of the molten aluminum alloy. The highest fluidity lengths for the copper-free (0% Cu) and 1% Cu-containing alloys were measured as 17.6 cm and 17.0 cm, respectively, at 750 °C. In contrast, in the alloy containing 2.5% Cu, the highest fluidity distance was obtained at 725 °C (15.7 cm) due to the widening of the solidification temperature range and the increase in viscous resistance.

2. An inversely proportional relationship was identified between the fluidity length and the mass per unit length (g/cm). Depending on the high specific gravity of copper and the filling characteristics of the mold cross-section, the sample containing 2.5% Cu, which had the shortest fluidity distance at 700 °C, exhibited the highest mass per unit length value of 5.52 g/cm.

3. The needle-like and plate-like Fe-Mn-rich intermetallic phases observed in the undoped secondary aluminum alloy evolved into a eutectic-dendritic network morphology in the interdendritic regions with the addition of copper. When the copper content in the melt was increased to 2.5%, the volumetric density of Cu-rich image (image eutectic phase) and complex intermetallic precipitates increased significantly during the final stage of solidification.

4. In addition to the Fe-Mn impurities originating from the dross, solid-solution strengthening within the matrix due to the increased copper content and the inhibition of dislocation movement by hard intermetallic phases precipitated at grain boundaries positively affected the microhardness values. The average hardness of image HV0.5 in the undoped alloy increased to image HV0.5 with the addition of 1% Cu and reached a maximum level of image HV0.5 with the addition of 2.5% Cu.

5. The findings demonstrate that aluminum dross waste, which is of critical importance from both environmental and economic perspectives, can be transformed into value-added casting materials through appropriate copper alloying and process temperature optimization.

ACKNOWLEDGMENT

This study did not received funding and authors declare there is no conflict of interest with any other parties.

REFERENCES

[1] K. Modalavalasa ve K. P. R. Ayyagari, "Aluminum dross: aluminum metal recovery and emerging applications", *J Mater Cycles Waste Manag*, c. 26, sy. 4, ss. 1874-1894, Tem. 2024, doi: 10.1007/s10163-024-01948-0.

[2] E. David ve J. Kopac, "Aluminum recovery as a product with high added value using aluminum hazardous waste", *Journal of Hazardous Materials*, c. 261, ss. 316-324, Eki. 2013, doi: 10.1016/j.jhazmat.2013.07.042.

[3] Y. Liu, X. Chen, S. Zhao, ve G. Wang, "Secondary Aluminum Dross: A Review on Sustainable Treatment Strategies, Material Valorization, and Environmental Considerations", *J. Sustain. Metall.*, c. 12, sy. 2, ss. 994-1011, Nis. 2026, doi: 10.1007/s40831-025-01407-6.

[4] O. Manfredi, W. Wuth, ve I. Bohlinger, "Characterizing the physical and chemical properties of aluminum dross", *JOM*, c. 49, sy. 11, ss. 48-51, Kas. 1997, doi: 10.1007/s11837-997-0012-9.

[5] L. Xu, D. Zhang, Y. Liu, ve M. Chen, "Iron Recovery from Waste Copper Slag by Using Coal and Secondary Aluminum Dross as Co-Reductants", *JOM*, c. 74, sy. 5, ss. 2029-2036, May. 2022, doi: 10.1007/s11837-022-05218-y.

[6] A. Kudyba, S. Akhtar, I. Johansen, ve J. Safarian, "Valorization of Aluminum Dross with Copper via High Temperature Melting to Produce Al-Cu Alloys", *Materials*, c. 14, sy. 15, s. 4117, Tem. 2021, doi: 10.3390/ma14154117.

[7] Zayad M. Sheggaf, Sharafaddeen S. Wanis Ehzazat, ve Almabrouk A. Dhaw Esdeira3, "Fluidity of Aluminum Piston Alloy with Different Amount of Pouring Temperature", *jhas*, c. 8, sy. 3, ss. 31-36, Eyl. 2023, doi: 10.58916/jhas.v8i3.111.

[8] K. R. Ravi, R. M. Pillai, K. R. Amaranathan, B. C. Pai, ve M. Chakraborty, "Fluidity of aluminum alloys and composites: A review", *Journal of Alloys and Compounds*, c. 456, sy. 1-2, ss. 201-210, May. 2008, doi: 10.1016/j.jallcom.2007.02.038.

[9] J. Wannasin, D. Schwam, J. A. Yurko, C. Rohloff, ve G. Woycik, "Hot Tearing Susceptibility and Fluidity of Semi-Solid Gravity Cast Al-Cu Alloy", *SSP*, c. 116-117, ss. 76-79, Eki. 2006, doi: 10.4028/www.scientific.net/SSP.116-117.76.

[10] M. D. Sabatino, "FLUIDITY OF ALUMINIUM FOUNDRY ALLOYS".

[11] B. K. Kang ve I. Sohn, "Effects of Cu and Si Contents on the Fluidity, Hot Tearing, and Mechanical Properties of Al-Cu-Si Alloys", *Metall Mater Trans A*, c. 49, sy. 10, ss. 5137-5145, Eki. 2018, doi: 10.1007/s11661-018-4786-x.

[12] G. Mao, D. Liu, W. Gao, S. Liu, ve L. Zhong, "The effects of copper (Cu) or zinc (Zn) on fluidity of A357 alloy", *Materials Letters*, c. 304, s. 130733, Ara. 2021, doi: 10.1016/j.matlet.2021.130733.

[13] A. K. Dahle, S. Karlsen, ve L. Arnberg, "Effect of grain refinement on the fluidity of some binary Al—Cu and Al—Mg alloys", *International Journal of Cast Metals Research*, c. 9, sy. 2, ss. 103-112, Tem. 1996, doi: 10.1080/13640461.1996.11819649.

[14] J. A. Taylor, "Iron-Containing Intermetallic Phases in Al-Si Based Casting Alloys", *Procedia Materials Science*, c. 1, ss. 19-33, 2012, doi: 10.1016/j.mspro.2012.06.004.

[15] C. M. Dinnis, J. A. Taylor, ve A. K. Dahle, "As-cast morphology of iron-intermetallics in Al–Si foundry alloys", *Scripta Materialia*, c. 53, sy. 8, ss. 955-958, Eki. 2005, doi: 10.1016/j.scriptamat.2005.06.028.

[16] S. Capuzzi ve G. Timelli, "Preparation and Melting of Scrap in Aluminum Recycling: A Review", *Metals*, c. 8, sy. 4, s. 249, Nis. 2018, doi: 10.3390/met8040249.

[17] N. A. Belov, A. A. Aksenov, ve D. G. Eskin, *Iron in aluminum alloys: impurity and alloying element*. içinde Advances in metallic alloys, no. v. 2. London: Taylor & Francis, 2002.
[18] M. H. Abdelaziz, A. M. Samuel, H. W. Doty, V. Songmene, ve F. H. Samuel, "Mechanical Performance and Precipitation Behavior in Al-Si-Cu-Mg Cast Alloys: Effect of Prolonged Thermal Exposure", *Materials*, c. 15, sy. 8, s. 2830, Nis. 2022, doi: 10.3390/ma15082830.
[19] S. Sarker, M. S. Haque, Md. S. A. Alvy, ve Md. M. H. Abir, "The effects of solution heat treatment on the microstructure and hardness of an aluminum-4% copper alloy with added nickel and tin", *Journal of Alloys and Metallurgical Systems*, c. 4, s. 100042, Ara. 2023, doi: 10.1016/j.jalmes.2023.100042.
[20] A. E. Al-Rawajfeh, "INVESTIGATION OF COPPER ADDITION ON THE MECHANICAL PROPERTIES AND CORROSION RESISTANCE OF COMMERCIALLY PURE ALUMINUM," *Emirates Journal for Engineering Research*, Jan. 2009, [Online]. Available: http://citeseerx.ist.psu.edu/viewdoc/summary?doi=10.1.1.531.7047
[21] Y. M. Abdulsahib, "EFFECT OF COPPER ADDITION ON THE MICROSTRUCTURE AND MECHANICAL PROPERTIES OF Al-Si ALLOY," *DOAJ (DOAJ: Directory of Open Access Journals)*, vol. 7, no. 4, Jan. 2014, [Online]. Available: https://doaj.org/article/e520ae74ab4547438110eb7a22d71110